Potential of *Araucaria angustifolia* bark as adsorbent to remove gentian violet dye from aqueous effluents

Jordana Georgin, Fernanda Caroline Drumm, Patrícia Grassi, Dison Franco, Daniel Allasia and Guilherme Luiz Dotto

ABSTRACT

Araucaria angustifolia bark (AA-Bark), a waste generated in wood processing, was evaluated as a potential adsorbent to remove Gentian Violet (GV) dye from aqueous solutions. The AA-Bark presented an amorphous structure with irregular surface and was composed mainly of lignin and holocellulose. These characteristics indicated that the adsorbent contains available sites to accommodate the dye molecules. The GV adsorption on AA-Bark was favored at pH 8.0 with adsorbent dosage of 0.80 g L^{-1}. Pseudo-nth order model was adequate to represent the adsorption kinetics of GV on AA-Bark. A fast adsorption rate was verified, with the equilibrium being attained within 30 min. Equilibrium data were well represented by the Langmuir model. The maximum adsorption capacity was 305.3 mg g^{-1}. Adsorption was spontaneous, favorable and endothermic. AA-Bark was able to treat a simulated dye house effluent, reaching color removal values of 80%. An excellent performance was found in fixed bed experiments, where the length of the mass transfer zone was only 5.38 cm and the breakthrough time was 138.5 h. AA-bark can be regenerated two times using HNO_3 0.5 mol L^{-1}. AA-Bark can be used as a low-cost material to treat colored effluents in batch and fixed bed adsorption systems.

Key words | adsorbent, fixed bed, gentian violet, mass transfer zone, simulated effluent

Jordana Georgin
Daniel Allasia
Civil Engineering Post Graduation Program,
Federal University of Santa Maria,
97105-900, Santa Maria,
Brazil

Fernanda Caroline Drumm
Patrícia Grassi
Dison Franco
Guilherme Luiz Dotto (corresponding author)
Chemical Engineering Department,
Federal University of Santa Maria,
97105-900, Santa Maria,
Brazil
E-mail: *guilherme_dotto@yahoo.com.br*

INTRODUCTION

Wood processing wastes contain high amounts of organic matter, phenolic compounds and other substances, which can cause environmental problems. *Araucaria angustifolia* are dioecious trees 25–35 m tall, with a straight trunk and horizontal branches, and the crown becoming flat-topped with age. The barks are finely scaly, resinous and striated horizontally (Silba 1986). Barks of coniferous trees, including *Araucaria angustifolia*, correspond to 25% of the trunk volume, and consequently, are generated in large amounts during wood processing. Large quantities of these wastes are decomposed in landfills, generating toxic substances that can contaminate the soil and water bodies (Röder & Thornley 2018). These wastes are normally used for energy generation in boilers, as substrate for seedling production, and for wood fiber production. However, a considerable amount continues without application. In this sense, some efforts have been made in order to minimize these wastes, searching for alternative applications (Moreno *et al.* 2017; Cetiner & Shea 2018; Hossain *et al.* 2018).

In parallel, textile, leather and other industries are responsible for the generation of large volumes of colored effluents, which, if incorrectly treated, can be dangerous to the environment and human health (Khamparia & Jaspal 2017). It is estimated that there are more than 100,000 types of synthetic dyes, with an annual production of 700,000 tons worldwide (Al-Fawwaz & Abdullah 2016). Due to the toxicity, carcinogenicity and mutagenicity of these contaminants, several studies have been developed in order to improve the operations used for the treatment of dye-containing effluents (Mu & Wang 2016). Among these operations, adsorption has gained attention to treat colored effluents due to advantages like efficiency, low cost, ease of operation, low energetic requirements and good performance relative to other conventional techniques. The use of adsorption technology is preferred

doi: 10.2166/wst.2018.448

when the adsorbate concentration is in the range of mg L^{-1}. Adsorption operation for dye removal is particularly improved if low cost and available materials are used as potential adsorbents (Bonilla–Petriciolet *et al.* 2017).

In order to reduce the operational costs and disseminate the adsorption technology, several alternative adsorbents have been studied (Bonilla–Petriciolet *et al.* 2017). For instance, low cost and available materials from vegetable sources have been tested to remove dyes from aqueous solutions in the last 10 years. Some examples are apple peels (Jain & Jayaram 2010), papaya seeds (Weber *et al.* 2014), giombo persimmon seeds (Bretanha *et al.* 2016), rice husks (Franco *et al.* 2015), peanut shells (Georgin *et al.* 2016), grape wastes (Vanni *et al.* 2017), *Eragrostis plana* nees (Dotta-Filho *et al.* 2017), ouricuri fibers (Meili *et al.* 2017) and Pará chestnut husk (Georgin *et al.* 2018). Here, the potential of *Araucaria angustifolia* bark (AA-Bark) to remove Gentian Violet (GV) dye from aqueous solutions was investigated. As the majority of vegetable alternative adsorbents, AA-Bark is composed by lignin, cellulose and hemicellulose. These macromolecules confer different properties to AA-Bark. Lignin is responsible for the link between the cellulose fibers, increasing the resistance and rigidity of the adsorbent. Cellulose, hemicellulose and lignin contain functional groups that can be potential sorption sites, like OH, COH, COOH, COC, CH_2, CH_3 and others. It should be highlighted that AA-Bark was already used to produce carbonaceous materials, which in turn, were tested for removal of some dyes from aqueous media (Kyzas 2015). However, this work is proposed to investigate the potential of raw AA-Bark, in order to avoid processing costs.

This work aimed to verify the potential of raw *Araucaria angustifolia* bark, a waste generated in wood processing, as an adsorbent to remove GV dye from aqueous effluents. For this purpose, *Araucaria angustifolia* bark (AA-Bark) was prepared in powder form and characterized by several techniques. Batch adsorption experiments were performed under different experimental conditions. Adsorption kinetics, equilibrium and thermodynamics were studied. The potential of AA-Bark was also evaluated to treat a simulated dye house effluent. Finally, adsorption was carried out in a fixed bed operation. In the light of this idea, a synergistic eco-friendly effect can be attained; that is, the use of AA-Bark is an alternative to solve the solid wastes management of wood industries, and this material can be used to treat liquid effluents from textile industries.

MATERIALS AND METHODS

Obtainment and characterization of *Araucaria angustifolia* BARK (AA-bark)

Araucaria angustifolia barks were obtained from a wood processing industry located in southern Brazil (Passo Fundo-RS). Barks were ground in a knife mill and sieved, generating a powdered material with a particle size lower than 0.20 mm. The powder was then washed with an ethanol solution (20% v/v) at 70 °C for 40 min under constant agitation of 200 rpm. The washing was performed four times in order to remove the extractives. The wet material was then separated from the liquid by sedimentation for 30 min and oven dried at 60 °C for 6 h. A powdered material with a moisture content of $7.5 \pm 0.5\%$ (wet basis) was obtained. This material was named AA-Bark.

The AA-Bark adsorbent was characterized by several techniques. The extractive content was determined by the TAPPI T204 cm-97 method. The lignin content was determined by the TAPPI T222 om-02 method. The holocellulose content was determined according to Morais *et al.* (2010). The point of zero charge (pH_{PZC}) was obtained using the eleven point's method (Park & Regalbuto 1995). X-ray powder diffractometry (XRD) (Rigaku, Miniflex 300, Japan) was used to evaluate the structure of AA-Bark (Saygılı & Güzel 2016). The main functional groups of AA-Bark were identified by Fourier transform infrared spectroscopy (FT-IR) (Shimadzu, Prestige 21, Japan) (Silverstein *et al.* 2007). The AA-Bark surface was visualized by scanning electron microscopy (SEM) (Jeol, JSM-6610LV, Japan) (Goldstein *et al.* 1992).

Batch adsorption study

Batch adsorption experiments were performed using colored solutions of GV dye (color index 42555, molar weight of 407.98 g mol^{-1}, $\lambda_{max} = 590$ nm), which was furnished by INLAB (Brazil) with a purity of 96%. Dye solutions were prepared with distilled water and analytical grade reagents were used. A stock solution of GV (1.00 g L^{-1}) was prepared and stored in amber flasks, with the experiments being performed using consecutive dilutions of this solution. All adsorption experiments were realized in a thermostated agitator (Marconi, MA 093, Brazil) at 150 rpm.

- At first, the adsorbent dosage effect was investigated using 0.50, 0.80, 1.00, 1.50 and 2.00 g L^{-1}. The adsorbent was added in 100 mL of an aqueous solution (pH of 7.1)

containing 100 mg L^{-1} of GV dye. Solutions were stirred for 60 min at 298 K;

- Secondly, the pH effect (2.0, 4.0, 6.0, 7.0, 8.0 and 10.0) was evaluated using the best adsorbent dosage previously determined. pH values were adjusted with NaOH and HCl. The adsorbent was added to 100 mL of an aqueous solution containing 100 mg L^{-1} of GV dye, which was stirred for 60 min at 298 K;
- Then, kinetic curves were constructed using the best values of adsorbent dosage and pH above determined. The curves were obtained at initial GV concentrations of 50 mg L^{-1}, 100 mg L^{-1} and 200 mg L^{-1}. For each test, the adsorbent was added in 100 mL of a GV dye solution, which was stirred at 298 K. Samples were collected at 5, 10, 15, 20, 25, 30, 40, 50 and 60 min;
- Finally, equilibrium curves were obtained using the best values of adsorbent dosage and pH above determined. The curves were obtained at 298, 308, 318 and 328 K, with an initial GV concentration from 0 to 300 mg L^{-1}. For each assay, the adsorbent was added in 100 mL of a GV dye solution, which was stirred until the equilibrium.

For all experiments, the GV concentration in the liquid phase was measured by spectrophotometry at 590 nm (Shimadzu, UV mini 1240, Japan). Experiments were realized in replicate ($n = 3$) and blanks were performed in order to guarantee the data reproducibility. After each experiment, samples were centrifuged (Centribio, 80-2B, Brazil) at 4,000 rpm for 10 min to perform the solid-liquid separation. The dye removal percentage (R, %), adsorption capacity at any time (q_t (mg g^{-1})) and at equilibrium (q_e (mg g^{-1})), were calculated as follows:

$$R = \frac{(C_0 - C_e)}{C_0} 100 \quad (1)$$

$$q_t = \frac{(C_0 - C_t)}{W} V \quad (2)$$

$$q_e = \frac{(C_0 - C_e)}{W} V \quad (3)$$

where, C_0, C_t, C_e (mg L^{-1}) are the GV concentrations at $t = 0$, at any time and at equilibrium, respectively, W (g) is the adsorbent amount and V (L) is the volume of the solution.

From the kinetic viewpoint, the experimental curves of GV adsorption onto AA-Bark were fitted with the pseudo first-order (Lagergren 1898), pseudo second-order (Ho & Mckay 1998) and pseudo nth-order models (Alencar *et al.* 2012), respectively:

$$q_t = q_1(1 - \exp(-k_1 t)) \quad (4)$$

$$q_t = \frac{t}{(1/k_2 q_2^2) + (t/q_2)} \quad (5)$$

$$q_t = q_n - \frac{q_n}{[k_n (q_n)^{n-1} t(n-1) + 1]^{(1/(n-1))}} \quad (6)$$

where, k_1, k_2 and k_n are the rate constants of pseudo first-order, pseudo second-order and pseudo-nth order models, respectively in (min^{-1}), (g mg^{-1} min^{-1}) and (min^{-1} (g mg^{-1})$^{n-1}$), q_1, q_2 and q_n are the theoretical values for the adsorption capacity (mg g^{-1}) and n is the order of adsorption reaction.

Regarding the isotherm data, the obtained curves were represented using the Langmuir (Langmuir 1918) and Freundlich (Freundlich 1906) models, as follows:

$$q_e = \frac{q_m K_L C_e}{1 + (K_L C_e)} \quad (7)$$

$$q_e = K_F C_e^{1/n_F} \quad (8)$$

where, q_m is the maximum adsorption capacity (mg g^{-1}), K_L is the Langmuir constant (L mg^{-1}), K_F is the Freundlich constant (mg g^{-1})(mg L^{-1})$^{-1/nF}$ and $1/n_F$ is the heterogeneity factor. The equilibrium factor (R_L) was estimated as:

$$R_L = \frac{1}{1 + (K_L C_e)} \quad (9)$$

Thermodynamic parameters like Gibbs free energy change (ΔG^0, kJ mol^{-1}), enthalpy change (ΔH^0, kJ mol^{-1}) and entropy change (ΔS^0, kJ mol^{-1} K^{-1}) were also estimated based on the experimental data. For this purpose, the thermodynamic equilibrium constant (K_e) was estimated from the isotherm parameters and applied in the following equations (Anastopoulos & Kyzas 2016):

$$\Delta G^0 = -RT \ln(K_e) \quad (10)$$

$$\Delta G^0 = \Delta H^0 - T\Delta S^0 \quad (11)$$

$$\ln(K_e) = \frac{\Delta S^0}{R} - \frac{\Delta H^0}{RT} \quad (12)$$

where, T is the temperature (K) and R is 8.31×10^{-3} kJ mol^{-1} K^{-1}.

Fixed bed adsorption experiments

The fixed bed adsorption experiments were carried out in an acrylic column (height 25 cm and diameter 2.5 cm)

according to Franco *et al.* (2017). The experimental conditions of pH, temperature and initial dye concentration were determined according to the batch studies. The column was completed with 27.2 g of AA-Bark. Then, the GV solution (pH of 8.0 and $C_0 = 100$ mg L^{-1}) was pumped to the column at 5 mL min^{-1} by a peristaltic pump (AWG, Provitec, Brazil). Samples were collected at the column top each 5 min until bed saturation. GV concentration in the liquid phase was measured by spectrophotometry at 590 nm (Shimadzu, UV mini 1240, Japan). Experiments were carried out in triplicate ($n = 3$).

Fixed bed adsorption data were treated in order to find the breakthrough curve (C_t/C_0 *versus* t). The operational parameters such as breakthrough time (t_b) and exhaustion time (t_e) were obtained from this curve, considering $C_t/C_0 = 0.05$ and $C_t/C_0 = 0.95$, respectively. The length of the mass transfer zone (Z_m) was then calculated as (Suzuki 1990):

$$Z_m = Z\left(1 - \frac{t_b}{t_e}\right) \tag{13}$$

where, Z is the bed length (cm).

The maximum stoichiometric capacity of the column (q_{eq}) and the respective removal percentage (R) were obtained as (Suzuki 1990):

$$q_{eq} = \frac{QC_0}{m}\int_0^{t_{total}}\left(1 - \left(\frac{C_t}{C_0}\right)\right)dt \tag{14}$$

$$R = \frac{100}{t_{total}}\int_0^{t_{total}}\left(1 - \left(\frac{C_t}{C_0}\right)\right)dt \tag{15}$$

where, C_0 is the inlet GV concentration (mg L^{-1}), C_t is the GV concentration along the time (mg L^{-1}), m is the adsorbent amount (g), Q is the flow rate (L h^{-1}) and t_{total} is the total operation time (h). The values of $(1 - (C_t/C_0))$ were estimated by Origin (Origin Lab Corp., USA) software (Franco *et al.* 2017). To represent the adsorption dynamic profile, the Thomas (Thomas 1944) and Yoon–Nelson (Yoon & Nelson 1984) models were fitted to the experimental data:

$$\frac{C_0}{C_t} = 1 + \exp\left(\frac{k_{Th}q_{eq}m}{Q} - k_{Th}C_0t\right) \tag{16}$$

$$\frac{C_0}{C_t} = 1 + \exp\left(k_{YN}\tau - k_{YN}t\right) \tag{17}$$

where, k_{Th} is the constant rate of the Thomas model (L g^{-1} h^{-1}), q_{eq} is the equilibrium adsorption capacity from the Thomas model (mg g^{-1}), k_{YN} is the constant rate of the Yoon–Nelson model (h^{-1}) and τ is the time required for 50% adsorbate breakthrough from Yoon–Nelson model (h).

Fitting

The parameters of batch and fixed bed adsorption models were estimated by the minimization of the least squares function, using Statistic 9.1 software (Statsoft, USA). For the batch adsorption models, the fit quality was measured through determination coefficient (R^2), adjusted determination coefficient (R^2_{adj}), average relative error (*ARE*) and sum of squared errors (*SSE*). For the fixed adsorption models, determination coefficient (R^2), *SSE* and mean of squared errors (*MSE*) were used (Bonilla–Petriciolet *et al.* 2017).

Treatment of dye house effluent and regeneration

The potential of *Araucaria angustifolia* bark (AA-bark) to treat a real effluent was evaluated, simulating a dye house effluent from dyeing step (Table 1) (Georgin *et al.* 2018). 100 mL of dye house effluent was treated with adsorbent dosages of 0.8 and 5.0 g L^{-1}, under constant stirring of 150 rpm for 60 min at 328 K. Before and after treatment, the liquid effluents were scanned from 400 to 800 nm in a spectrophotometer. The color removal percentage was calculated by the ratio between the areas below the spectroscopic curves. The regeneration studies are presented in supplementary material (Figure S).

RESULTS AND DISCUSSION

Characteristics of *Araucaria angustifolia* bark

AA-Bark adsorbent presented 3.8% of extractive content, 27.8% of lignin and 68.4% of holocellulose. The lignocellulosic fraction contains functional groups, such as OH, COH, COOH, COC, CH_2, CH_3 and others that are able to interact with GV dye. These groups will be better identified in FT-IR analysis. The point of zero charge (pH_{PZC}) of

Table 1 | Chemical composition of the dye house effluent from the dyeing step

Compounds	λ_{max}	Concentration (mg L^{-1})
Gentian Violet	590	100
Methylene Blue	664	50
Malachite Green	615	50
NaCl	–	100
Na_2CO_3	–	100
pH	–	10.2

AA-Bark was 7.0 (Figure S1), indicating that under acid conditions the adsorbent is positively charged while, in basic media, the material is negatively charged.

The XRD pattern of AA-Bark is presented in the supplementary material (Figure S2). The XRD pattern is characterized by broad peaks from 10° to 30° and narrow peaks from 30° to 70°. The broad peaks from 10° to 30° are relative to the amorphous phase of AA-Bark, which can be attributed to the lignin content. The narrow peaks from 30° to 70° are relative to the crystalline regions, which can be assigned to the cellulose content. In this way, it can be verified that the adsorbent material presented characteristics of both phases, amorphous and crystalline.

FT-IR spectra of AA-bark before (black) and after the GV adsorption (red) are presented in supplementary material (Figure S3). AA-bark before adsorption (black line) presented several bands, indicating a complex structure of the material and the presence of different functional groups on the surface. The main bands were found at 3,434, 2,925, 1,612, 1,517, 1,446 and 1,056 cm^{-1}. The broad vibrational stretching at 3,434 cm^{-1} can be assigned to the O-H links of cellulose and lignin. The C-O bonds, probably of the carboxylic groups, can be verified at 2,925 cm^{-1}. At 1,162 cm^{-1}, the C = N link can be observed. The bands at 1,517 and 1,446 cm^{-1} are relative to the aromatic C = C links. The phenolic C-O link can be observed at 1,056 cm^{-1}. After adsorption (red line) no significant changes were observed. Furthermore, no links were formed or broken. This can be an indicative that the adsorption was physical in nature.

The SEM images of AA-bark at different magnifications are presented in Figure 1. Figure 1(a) confirms that the adsorbent is a fine particulate material. In Figures 1(b) and 1(c), it can be seen that AA-bark has an irregular and heterogeneous surface, with cavities and protuberances. Figure 1(d) shows that the material surface contains cracks and voids. These characteristics are favorable for GV adsorption, since they allow the penetration of the colored liquid in the external and internal structure of the adsorbent.

Effects of AA-bark dosage and pH

The adsorbent dosage effect on the GV adsorption onto AA-bark is presented in Figure 2(a). The GV removal percentage (R) increased from 58 to 92% when the adsorbent dosage was increased from 0.5 to 2.0 g L^{-1}. This is due to the increase in the total number of adsorption sites. Evidently, the adsorption capacity values (q) presented an inverse dependence. The q values decreased from 83.4 to 51.6 mg g^{-1} when the adsorbent dosage was increased from 0.5 to 2.0 g L^{-1}. This behavior was due to the overlap of adsorption sites. The same trend in relation to q and R was found by Georgin *et al.* (2018) in the biosorption of Crystal Violet and Methylene Blue dyes onto Pará chestnut husk. The intersection of the blue and black curves in Figure 3 was at 0.8 g L^{-1}. The use of this dosage furnished reasonable values of R and q. Consequently, 0.8 g L^{-1} was selected as the more adequate value of adsorbent dosage.

Figure 2(b) shows the effect of pH on the GV adsorption onto AA-bark. It was observed that the pH increase from 2.0 to 8.0 provoked a strong increase in the adsorption capacity from 45 to 85 mg g^{-1}. A new increase from 8.0 to 10.0 presented no effect. This occurred because at pH values higher than 7.0, the AA-bark surface is negatively charged. In parallel, the GV dye is in its ionized form (as a cation) at pH values higher than 4.6. Then, under basic conditions, the GV cation is attracted by the negative surface of the AA-bark. A similar trend was found by Brião *et al.* (2017) in the adsorption of Crystal Violet dye on a modified zeolite. They found that the pH increase from 2.0 to 8.0 caused a strong increase in the CV removal percentage, attaining 78% at pH of 8.0. Based on these results, pH of 8.0 was selected to perform the subsequent experiments.

Adsorption kinetic profile

The adsorption kinetic profile of GV dye on the AA-bark adsorbent is presented in Figure 3. It was verified that, independent of the initial dye concentration, the GV adsorption was fast, with the equilibrium being attained at around 30 min. This is favorable for adsorption processes, since the treatment of colored effluents can be performed efficiently in short time intervals.

Pseudo first-order, pseudo second-order and pseudo nth-order models were fitted with the experimental kinetic data in order to better understand the kinetic profile. The results are presented in Table 2. Comparing the values of R^2, R^2_{adj}, ARE and SSE (Table 2), it can be concluded that the pseudo nth-order model was the more adequate to represent the experimental kinetic curves. The better performance of this model is also verified by the q_n values, which were close to the experimental values ($q_e(exp)$). The q_n values increased with the initial concentration, confirming that the adsorption capacity was higher at higher initial GV concentrations. The k_n parameter increased with the initial concentration, showing that the adsorption was faster at higher concentrations. The n values were between 0.77 and 0.79, showing that the reaction order is not an integer number. This behavior coupled with the

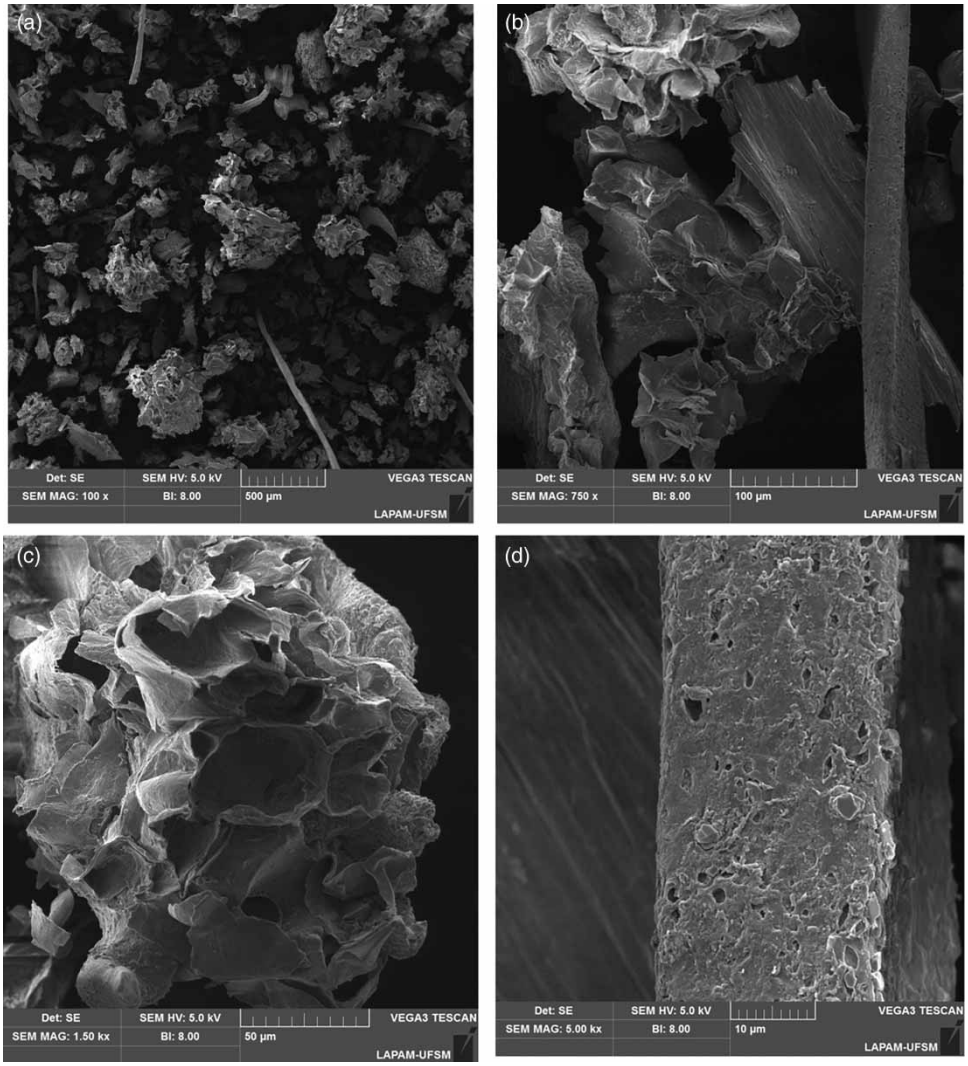

Figure 1 | SEM images of AA-bark (a) ×100, (b) ×750, (c) ×5,000 and (d) ×5,000.

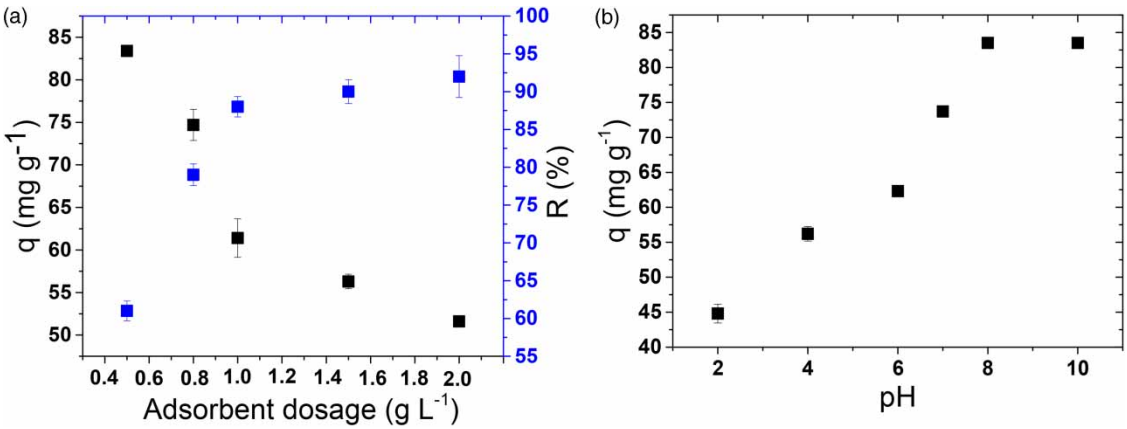

Figure 2 | (a) Adsorbent dosage effect for the system GV dye and AA-bark adsorbent ($C_o = 100$ mg L^{-1}, $T = 298$ K, $t = 60$ min, $V = 100$ mL, pH = 7.1 and stirring rate = 150 rpm); (b) pH effect for the system GV dye and AA-bark adsorbent ($C_o = 100$ mg L^{-1}, $T = 298$ K, $t = 60$ min, $V = 100$ mL, adsorbent dosage = 0.8 g L^{-1} and stirring rate = 150 rpm).

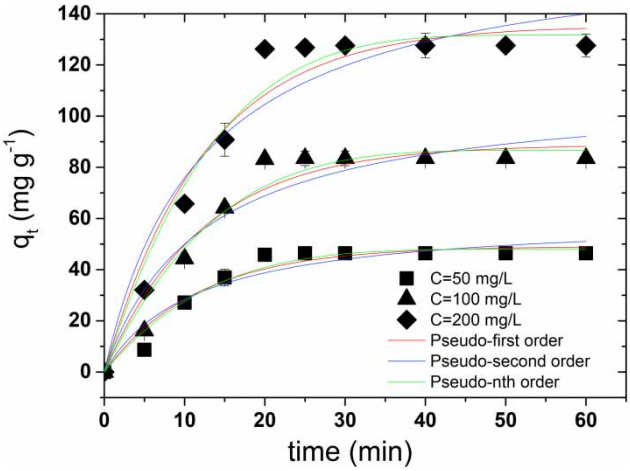

Figure 3 | Adsorption kinetic curves of GV onto AA-bark adsorbent ($T = 298$ K, adsorbent dosage = 0.8 g L^{-1}, pH = 8.0, stirring rate = 150 rpm).

good statistical indicators (R^2, R^2_{adj}, ARE and SSE) justifies the use of pseudo nth-order model to represent the GV adsorption onto AA-bark adsorbent.

Equilibrium isotherms and thermodynamics

Isotherms curves for the GV adsorption onto AA-bark are presented in Figure 4. It was observed that all isotherms were favorable. During the entire concentration range, the q_e values increased with C_e. Independent of the temperature, the plateau was not attained in this concentration range. This indicates that the AA-bark adsorption sites were not completely occupied, and consequently the material has additional potential to adsorb GV. Furthermore, it was verified that the adsorption capacity was favored by the temperature increase. This phenomenon is generally attributed to the thermal collision effect or modifications in the adsorbent structure at higher temperatures, for example, swelling effect (Bonilla–Petriciolet *et al.* 2017).

Langmuir and Freundlich models were used to represent the equilibrium experimental data. The results are presented in Table 3. Both models presented interesting values of the statistical indicators. However, analyzing in detail and considering that the Langmuir model is based

Table 2 | Kinetic parameters for GV adsorption onto AA-bark adsorbent

	Initial GV concentration (mg L^{-1})		
Model	**50**	**100**	**200**
Pseudo-first order			
q_1 (mg g^{-1})	49.08 ± 2.48	88.81 ± 4.79	135.36 ± 6.45
k_1 (min^{-1})	0.086 ± 0.014	0.082 ± 0.014	0.080 ± 0.012
R^2	0.9539	0.9516	0.9615
R^2_{adj}	0.9482	0.9455	0.9567
ARE (%)	15.34	15.06	10.55
SSE	126.50	436.611	772.73
Pseudo-second order			
q_2 (mg g^{-1})	60.66 ± 6.49	110.79 ± 12.47	168.41 ± 16.97
$k_2 \times 10^4$ (g mg^{-1} min^{-1})	14.6 ± 6.6	7.4 ± 3.4	4.9 ± 2.0
R^2	0.9222	0.9206	0.9342
R^2_{adj}	0.9125	0.9107	0.9259
ARE (%)	19.33	15.06	10.55
SSE	213.82	715.48	1,322.61
Pseudo-nth order			
q_n (mg g^{-1})	48.05 ± 2.20	86.66 ± 4.21	131.68 ± 5.39
k_n (min^{-1} (g mg^{-1})$^{n-1}$)	0.17 ± 7.9 × 10^{-5}	0.20 ± 9.2 × 10^{-5}	0.22 ± 0.01
n	0.786 ± 0.039	0.776 ± 0.034	0.775 ± 0.037
R^2	0.9660	0.9646	0.9732
R^2_{adj}	0.9563	0.9545	0.9656
ARE (%)	12.94	12.69	8.53
SSE	93.28	318.66	537.44
q_e*(exp)* (mg g^{-1})	46.5	83.4	127.0

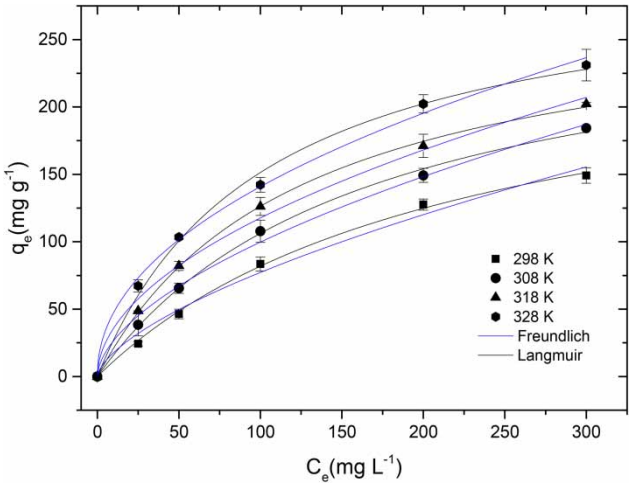

Figure 4 | Adsorption isotherm curves of GV onto AA-bark adsorbent (adsorbent dosage = 0.8 g L^{-1}, pH = 8.0).

on physical assumptions, while the Freundlich is an empirical model, the Langmuir model was selected to represent the adsorption isotherms. The q_m parameter was directly proportional with the temperature, with the maximum value being 305.3 mg g^{-1}, attained at 328 K. For comparison, Jain & Jayaram (2010) applied wood apple shells to remove basic dyes from aqueous media and found an adsorption capacity of 130 mg g^{-1}, using 1 g L^{-1} of adsorbent at pH 10 and 305 K. Weber *et al.* (2014) used papaya seeds to adsorb pharmaceutical dyes. They found an adsorption capacity of 51 mg g^{-1} at pH 2.5 and 298 K. Bretanha *et al.* (2016) evaluated Toluidine Blue adsorption on Giombo persimmon seeds and found the adsorption capacity to be around 37 mg g^{-1} at pH 8.0 and 298 K. Modified chitin was used to remove Methylene Blue from aqueous solutions and the adsorption capacity was around 25 mg g^{-1} at pH 10 and 298 K (Franco *et al.* 2015). Activated carbon from peanut shell was used by Georgin *et al.* (2016) to adsorb organic dyes. They found an adsorption capacity of 284.5 mg g^{-1} at pH 2.5 and 298 K. Vanni *et al.* (2017) used powdered grape seeds (PGS) as an alternative biosorbent to remove pharmaceutical dyes from aqueous media and found a biosorption capacity of 599.5 mg g^{-1} at pH 1.0 and 328 K. Dotta-Filho *et al.* (2017) used *Eragrostis plana* Nees to remove Crystal Violet from aqueous solutions and found an adsorption capacity of 76 mg g^{-1} at pH 8.0 and 333 K. Ouricuri fiber was used by Meili *et al.* (2017) to adsorb methylene blue. They found adsorption capacity of 31.7 mg g^{-1} at pH 5.5 and 298 K. In the work of Georgin *et al.* (2018), the biosorption of cationic dyes by Pará chestnut husk was studied. They found an adsorption capacity of 83.8 mg g^{-1} using an adsorbent dosage of 0.5 g L^{-1} and 298 K. Comparing now the abovementioned values of adsorption capacity from different adsorbents and dyes, it is possible to conclude that the value found in this work (305.3 mg g^{-1}) is relatively high. This indicates that AA-bark is a promising candidate to remove dyes from aqueous media. Regarding

Table 3 | Isotherm parameters for GV adsorption onto AA-bark adsorbent

	Temperature (K)			
Model	**298**	**308**	**318**	**328**
Freundlich				
K_f (mg g^{-1}) (mg L^{-1})$^{-1/nf}$	4.1 ± 1.2	7.1 ± 1.2	11.0 ± 1.9	16.0 ± 1.8
1/nf	1.56 ± 0.14	1.74 ± 0.10	1.94 ± 0.13	2.11 ± 0.10
R^2	0.9882	0.9949	0.9936	0.9960
R^2_{adj}	0.9852	0.9937	0.9920	0.9950
ARE (%)	11.20	5.87	5.92	3.51
SSE	204.12	121.14	185.72	120.03
Langmuir				
q_m (mg g^{-1})	262.6 ± 13.1	282.2± 5.9	280.8 ± 11.3	305.3± 14.1
K_L (L mg^{-1})	0.0045 ± 0.0004	0.0081 ± 0.0003	0.0061 ± 0.0005	0.0098 ± 0.0011
R_L	0.425	0.291	0.353	0.254
R^2	0.9985	0.9993	0.9984	0.9967
R^2_{adj}	0.9982	0.9992	0.9980	0.9959
ARE (%)	3.99	18.11	16.07	4.15
SSE	24.90	18.43	37.00	147.66

now the R_L parameter (Table 3), the values were between 0 and 1, indicating a favorable adsorption process.

For the thermodynamic calculations, the Langmuir parameters were considered to estimate K_e, and then compute ΔG^0, ΔH^0 and ΔS^0. The adsorption system of AA-bark/GV dye presented ΔG^0 values from −4.8 to −3.7 kJ mol^{-1}. These negative values attest to the process spontaneity. The ΔS^0 value was 0.033 kJ mol^{-1} K^{-1}. This positive value indicated that some rearrangements occurred on the AA-bark surface during GV adsorption. The ΔH^0 value was 6.3 kJ mol^{-1}. The positive signal confirms that the GV adsorption onto AA-bark was endothermic in nature. The low magnitude of ΔH^0 suggests that physisorption occurred between GV and AA-bark (Bonilla–Petriciolet *et al.* 2017).

The probable interaction mechanism was proposed on the basis in FTIR (Figure S3), pH effect (Figure 2), desorption studies (Figure S), thermodynamic parameters and adsorbent/adsorbate characteristics. According to the FTIR, no links were formed or broken after adsorption, indicating a physical nature. This fact is confirmed by the low ΔH^0 value. Physical adsorption can be due to electrostatic interactions, hydrogen bonds, dipole-dipole or Van der Waals interactions. It was found that the GV adsorption onto AA-bark was extremely pH dependent. This fact, coupled with the cationic nature of GV and the point of zero charge of the AA-bark, indicated that electrostatic interactions were involved in the adsorption. Electrostatic interactions can be corroborated since desorption was efficient in acid media.

Fixed bed adsorption

Fixed bed adsorption experiments were performed to verify the potential of AA-bark to be applied in continuous systems. The results are presented in Figure 5. The good performance of AA-bark to treat the colored liquid in a continuous manner can be seen. The breakthrough curve reveals that the system can operate for 138.5 h without the necessity of regeneration. Until 138.5 h, the liquid at the column top was practically transparent, as clearly demonstrated in Figure 5. After the breakthrough time (t_b), the curve was strongly inclined, attaining the exhaustion time (t_b) at 176.5 h. This strong inclination provided a short length of mass transfer zone ($Z_m = 5.38$ cm), which is extremely interesting for scale-up. The values of R and q_{eq} were also satisfactory. For these reasons, AA-bark has potential to be applied in continuous adsorption processes.

The breakthrough curve was represented by the Thomas and Yoon–Nelson models. The results are presented in Table 4. Based on the high values of R^2 and low values of

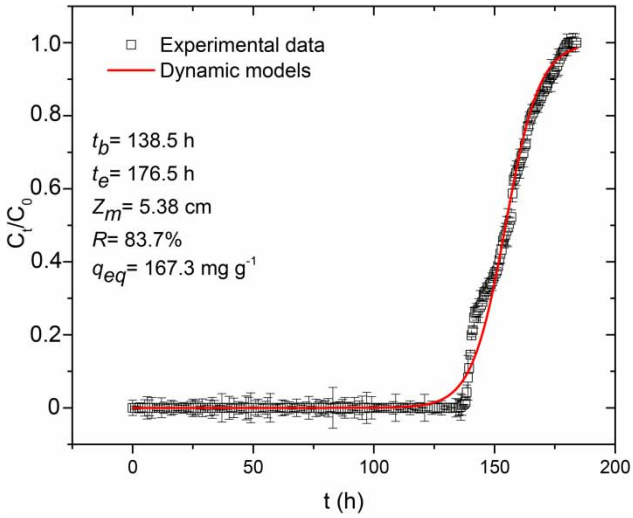

Figure 5 | Breakthrough curve of GV adsorption onto AA-bark adsorbent (solution pH = 8.0, $Q = 5$ mL min^{-1}, $C_0 = 100$ mg L^{-1}).

SSE and *MSE*, it can be seen that both models were able to represent the breakthrough curve. The Thomas model was able to predict the stoichiometry adsorption capacity (q_{eq}) with a deviation of only 1.9%. The Yoon-Nelson model in turn was able to predict τ with variation of only 0.26%.

Treatment of dye house effluent

The potential of AA-bark to treat a simulated dye house effluent was tested. The effluent composition is presented in Table 1. The spectra of untreated and treated effluent are

Table 4 | Dynamic parameters for GV adsorption onto AA-bark adsorbent

Model	Parameter values
Thomas	
k_{Th} (L g^{-1} h^{-1})	1.26
q_{eq} (mg g^{-1})	170.5
$q_{eq(exp)}$ (mg g^{-1})	167.3
R^2	0.9942
SSE	0.18
MSE	7.7×10^{-4}
Yoon-Nelson	
k_{YN} (h^{-1})	0.126
τ (h)	154.6
$\tau_{(exp)}$ (h)	155.0
R^2	0.9942
SSE	0.18
MSE	7.7×10^{-4}

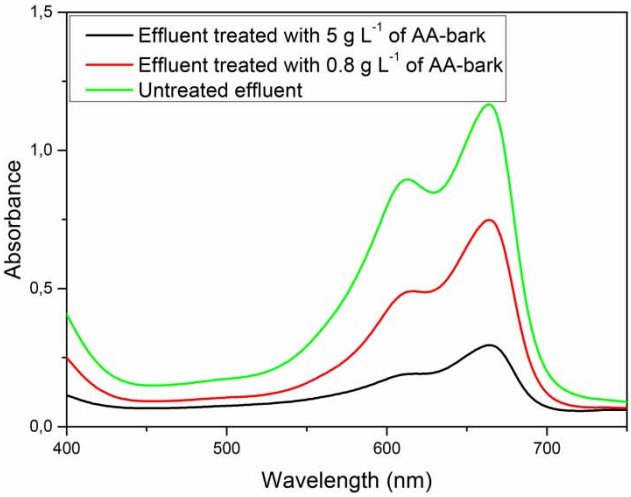

Figure 6 | Visible spectra of dye house effluents before and after the adsorption with AA-bark.

depicted in Figure 6. It was found that the use of 0.8 g L^{-1} was not sufficient to provide a suitable treatment, since the curve was little amortized (red curve). Then, an adsorbent dosage of 5 g L^{-1} was tested. The treatment with 5 g L^{-1} furnished color removal percentage of around 80%, which was considered satisfactory. In this way, it can be affirmed that AA-bark has potential to treat dye house effluents.

CONCLUSION

The potential of *Araucaria angustifolia* bark (AA-Bark) as an adsorbent to remove GV dye from aqueous solutions was investigated in batch and continuous adsorption operations. From the discontinuous batch studies, it was found that GV adsorption was favored at pH of 8.0 and adsorbent dosage of 0.8 g L^{-1}. Adsorption kinetics were fast, with the equilibrium being attained within 30 min. The pseudo-nth order model was adequate to represent the kinetic curves. Equilibrium isotherms were well represented by the Langmuir model, with a maximum adsorption capacity of 305.3 mg g^{-1} attained at 328 K. Adsorption of GV onto AA-bark was a spontaneous, favorable, endothermic and physical process. The fixed bed analysis revealed that the system can operate for 138.5 h without the necessity of regeneration. Also a short length of mass transfer zone ($Z_m = 5.38$ cm) was obtained. The Thomas and Yoon-Nelson models were able to represent the adsorption dynamics. AA-bark can be regenerated twice using HNO_3 0.5 mol L^{-1}, maintaining the same adsorption capacity. AA-bark was suitable to treat a simulated dye house effluent containing various dyes and inorganic salts, presenting a color removal percentage of 80%. Based on this evaluation, it can be stated that AA-bark is an alternative adsorbent able to treat colored dye house effluents in batch and continuous adsorption systems.

REFERENCES

Alencar, W. S., Lima, E. C., Royer, B., dos Santos, B. D., Calvete, T., da Silva, E. A. & Alves, C. N. 2012 Application of aqai stalks as biosorbents for the removal of the dye Procion Blue MX-R from aqueous solution. *Separation Science and Technology* **47** (3), 513–526.

Al-Fawwaz, A. T. & Abdullah, M. 2016 Decolorization of methylene blue and malachite green by immobilized desmodesmus sp. Isolated from North Jordan. *International Journal of Environmental Science and Development* **7** (2), 95–99.

Anastopoulos, I. & Kyzas, G. Z. 2016 Are the thermodynamic parameters correctly estimated in liquid-phase adsorption phenomena? *Journal of Molecular Liquids* **218** (1), 174–185.

Bonilla–Petriciolet, A., Mendoza–Castillo, D. I. & Reynel–Ávila, H. E. 2017 *Adsorption Processes for Water Treatment and Purification*. Springer International Publishing, Berlin, Germany.

Bretanha, M. S., Dotto, G. L., Vaghetti, J. C. P., Dias, S. L. P., Lima, E. C. & Pavan, F. A. 2016 Giombo persimmon seed (GPS) an alternative adsorbent for the removal Toluidine Blue dye from aqueous solutions. *Desalination and Water Treatment* **57** (58), 28474–28485.

Brião, G. V., Jahn, S. L., Foletto, E. L. & Dotto, G. L. 2017 Adsorption of crystal violet dye onto a mesoporous ZSM-5 zeolite synthetized using chitin as template. *Journal of Colloid and Interface Science* **508** (1), 313–322.

Cetiner, I. & Shea, A. D. 2018 Wood waste as an alternative thermal insulation for buildings. *Energy & Buildings* **168** (1), 374–384.

Dotta-Filho, E. C., Mazzocato, A. C., Dotto, G. L., Thue, P. S. & Pavan, F. A. 2017 *Eragrostis plana* Nees as a novel eco-friendly adsorbent for removal of crystal violet from aqueous solutions. *Environmental Science Pollution Research* **24** (1), 19909–19919.

Franco, D. S. P., Piccin, J. S., Lima, E. C. & Dotto, G. L. 2015 Interpretations about methylene blue adsorption by surface modified chitin using the statistical physics treatment. *Adsorption* **21** (1), 557–564.

Franco, D. S. P., Tanabe, E. H. & Dotto, G. L. 2017 Continuous adsorption of a cationic dye on surface modified rice husk: statistical optimization and dynamic models. *Chemical Engineering Communications* **204** (1), 625–634.

Freundlich, H. 1906 Uber die adsorption in losungen. *Zeitschrift fur Physikalische Chemie* **57** (A), 358–471.

Georgin, J., Dotto, G. L., Mazutti, M. A. & Foletto, E. L. 2016 Preparation of activated carbon from peanut shell by conventional pyrolysis and microwave irradiation-pyrolysis

to remove organic dyes from aqueous solutions. *Journal of Environmental Chemical Engineering* **4** (1), 266–275.

Georgin, J., Marques, B. S., Peres, E. C., Allasia, D. & Dotto, G. L. 2018 Biosorption of cationic dyes by Pará chestnut husk (*Bertholletia excelsa*). *Water Science and Technology* **77** (6), 1612–1621.

Goldstein, J. I., Newbury, D. E., Echil, P., Joy, D. C., Romig Jr., A. D., Lyman, C. E., Fiori, C. & Lifshin, E. 1992 *Scanning Electron Microscopy and X-ray Microanalysis*. Plenum Press, New York, USA.

Ho, Y. S. & Mckay, G. 1998 Kinetic models for the sorption of dye from aqueous solution by wood. *Process Safety and Environmental Protection* **76** (B2), 183–191.

Hossain, M. U., Wang, L., Yu, I. K. M., Tsang, D. C. W. & Poon, C. S. 2018 Environmental and technical feasibility study of up cycling wood waste into cement-bonded particle board. *Construction and Building Materials* **173** (1), 474–480.

Jain, S. & Jayaram, R. V. 2010 Removal of basic dyes from aqueous solution by low-cost adsorbent: wood apple shell (*Feronia acidissima*). *Desalination* **250** (3), 921–927.

Khamparia, S. & Jaspal, D. K. 2017 *Xanthium strumarium L.* seed hull as a zero cost alternative for Rhodamine B dye removal. *Journal of Environmental Management* **197** (1), 498–506.

Kyzas, G. Z. 2015 *Green Adsorbents*. Bentham Science, Sharjah, UAE.

Lagergren, S. 1898 About the theory of so-called adsorption of soluble substances. *Kungliga Svenska Vetenskapsakademiens* **24** (4), 1–39.

Langmuir, I. 1918 The adsorption of gases on plane surfaces of glass, mica and platinum. *Journal of the American Chemical Society* **40** (9), 1361–1403.

Meili, L., Silva, T. S., Henrique, D. C., Soletti, J. I., Vieira de Carvalho, S. H., Fonseca, E. J. S., Almeida, A. R. F. & Dotto, G. L. 2017 Ouricuri (*Syagrus coronata*) fiber: a novel biosorbent to remove methylene blue from aqueous solutions. *Water Science and Technology* **75** (1), 106–114.

Morais, J. P. S., Rosa, M. F. & Marconcini, J. M. 2010 *Procedures for Lignocellulosic Analyses*. EMBRAPA, Campina Grande, Brazil.

Moreno, A. I., Font, R. & Conesa, J. A. 2017 Combustion of furniture wood waste and solid wood: kinetic study and evolution of pollutants. *Fuel* **192** (1), 169–177.

Mu, B. & Wang, A. 2016 Adsorption of dyes onto palygorskite and its composites: a review. *Journal of Environmental Chemical Engineering* **4** (1), 1274–1294.

Park, J. & Regalbuto, J. R. 1995 A simple, accurate determination of oxide PZC and the strong buffering effect of oxide surfaces at incipient wetness. *Journal of Colloid and Interface Science* **175** (1), 239–252.

Röder, M. & Thornley, P. 2018 Waste wood as bioenergy feedstock, climate change impacts and related emission uncertainties from waste wood based energy systems in the UK. *Waste Management* **74** (1), 241–252.

Saygılı, H. & Güzel, F. 2016 High surface area mesoporous activated carbon from tomato processing solid waste by zinc chloride activation: process optimization, characterization and dyes adsorption. *Journal of Cleaner Production* **113** (1), 995–1004.

Silba, J. 1986 *Encyclopaedia Coniferae*. New York Botanical Garden, New York, USA.

Silverstein, R. M., Webster, F. X. & Kiemle, D. J. 2007 *Spectrometric Identification of Organic Compounds*. John Wiley & Sons, New York, USA.

Suzuki, M. 1990 *Adsorption Engineering*. Kodansha, Tokyo, Japan.

Thomas, H. C. 1944 Heterogeneous ion exchange in a flowing system. *Journal of the American Chemical Society* **66** (1), 1466–1664.

Vanni, G., Escudero, L. B. & Dotto, G. L. 2017 Powdered grape seeds (PGS) as an alternative biosorbent to remove pharmaceutical dyes from aqueous solutions. *Water Science and Technology* **76** (5), 1177–1187.

Weber, C. T., Collazzo, G. C., Mazutti, M. A., Foletto, E. L. & Dotto, G. L. 2014 Removal of hazardous pharmaceutical dyes by adsorption onto papaya seeds. *Water Science and Technology* **70** (1), 102–107.

Yoon, Y. H. & Nelson, J. H. 1984 Application of gas adsorption kinetics: part 1: a theoretical model for respirator cartridge service time. *American Industrial Hygiene Association Journal* **45** (8), 509–516.

First received 3 July 2018; accepted in revised form 12 October 2018. Available online 23 October 2018